

Broken-Symmetry Density Functional Theory Investigation on Bis-Nitronyl Nitroxide Diradicals: Influence of Length and Aromaticity of Couplers

Md. Ehesan Ali and Sambhu N. Datta*

Department of Chemistry, Indian Institute of Technology-Bombay, Powai, Mumbai 400076, India

Received: December 6, 2005; In Final Form: January 4, 2006

A series of nitronyl nitroxide (NN) diradicals with linear conjugated couplers and another series with aromatic couplers have been investigated by the broken-symmetry (BS) DFT approach. The overlap integral between the magnetically active orbitals in the BS state has been explicitly computed and used for the evaluation of the magnetic exchange coupling constant (J). The calculated J values are in very good agreement with the observed values in the literature. The magnitude of J depends on the length of the coupler as well as the conformation of the radical units. The aromaticity of the spacer decreases the strength of the exchange coupling constant. The SOMO–SOMO energy splitting analysis, where SOMO stands for the singly occupied molecular orbital, and the calculation of electron paramagnetic resonance (EPR) parameters have also been carried out. The computed hyperfine coupling constants support the intramolecular magnetic interactions. The nature of magnetic exchange coupling constant can also be predicted from the shape of the SOMOs as well as the spin alternation rule in the unrestricted Hartree–Fock (UHF) treatment. It is found that π -conjugation along with the spin-polarization plays the major role in controlling the magnitude and sign of the coupling constant.

1. Introduction

The search for new magnetic materials based on organic paramagnetic molecules has recently generated a tremendous interest. The synthesis and characterization of the first pure organic radical based magnetic material, β -crystal phase of *p*-nitrophenyl nitronyl nitroxide,^{1,2} triggered the research in this field. Till now a large number of nitronyl nitroxide (NN) based diradicals has been experimentally investigated.³

The intramolecular magnetic exchange coupling constant, as well as the intermolecular interaction that depends on the structure and the nature of a molecular crystal, control the magnetic properties of a molecule-based magnetic material. An estimate of the intramolecular exchange coupling constant is necessary prior to synthesizing a successful magnetic material based on organic diradicals or transition metal complexes. The recent development of computational techniques and theoretical methodologies has enabled the prediction of magnetic properties of the precursors.⁴ Here we report the results of the study of a series of nitronyl nitroxide based diradicals with different conjugated magnetic couplers.

The magnetic interaction between two radical centers normally depends on the distance and the nature of the coupler. Turek et al.⁵ have investigated a series of *m*-phenylene couplers and shown that the influence of spin polarization and molecular conformation controls the exchange coupling constant. Castell et al.⁶ have performed ab initio computations on model compounds of bis(nitronyl) and bis(imino) nitroxides with varying dihedral angles. They have noticed that even at the orthogonal position the ground state is a singlet. Barone et al.⁷ have theoretically investigated bis(imino) nitroxide and concluded that most of the spin density along the O–N–C–N moiety of each monomeric unit can be attributed to the unpaired electron in the singly occupied molecular orbital. This implies

that a coupler that is extensively conjugated can give rise to a strong magnetic interaction between the monomeric radical centers. This very important theme forms the background of the present work. Zeissele et al.^{8a} have synthesized a nitronyl nitroxide diradical with the ethylene coupler, which shows a very high exchange coupling constant.

In a recent communication to this journal,⁹ we have theoretically verified that a very strong intramolecular magnetic interaction is indeed provided by an ethylene coupler. In the present work we establish that the strength of the magnetic interaction decreases with the increase in size of the conjugated coupler in a quantitative way, and also with the extent of aromaticity of the ring coupler. With this aim, we have studied a series of NN diradicals with different magnetic couplers: No coupler (1), ethylene coupler (2), 1,4 butadiene coupler (3), 1,6-hexatriene coupler (4), *p*-phenylene coupler (5), 2,6-pyridine coupler (6), *m*-phenylene coupler (7), 2,5-furan coupler (8), 2,5-pyrrole coupler (9), and 2,5 *m*-thiophene coupler (10) (Figure 1). All the couplers are π -conjugated molecules.

The magnetic couplings are generally found to arise from spin polarization and spin delocalization.¹⁰ Lahti et al.¹¹ have investigated a large number of π -conjugated couplers. They have noticed that most of the spin density is localized on the two-singly occupied σ orbitals (SOMOs) centered on the radical atoms. The large spin population polarizes the π electrons near the radical center. The total π spin density sums to zero over all sites in the singlet state, but the individual sites may be polarized to have positive or negative spin densities. The spin polarization effect plays a major role in controlling the nature of the coupling. The presence of nonbonding molecular orbitals (NBMOs) in organic diradicals makes it difficult to properly evaluate the energy difference between the lowest spin-states. The expected ground state spin may be predicted either by molecular orbital (MO) calculation or by a valence bond (VB) treatment. In the simple MO model, Hund's multiplicity rules are often applied to molecules having degenerate or nondegen-

* Corresponding author. E-mail: sndatta@chem.iitb.ac.in.

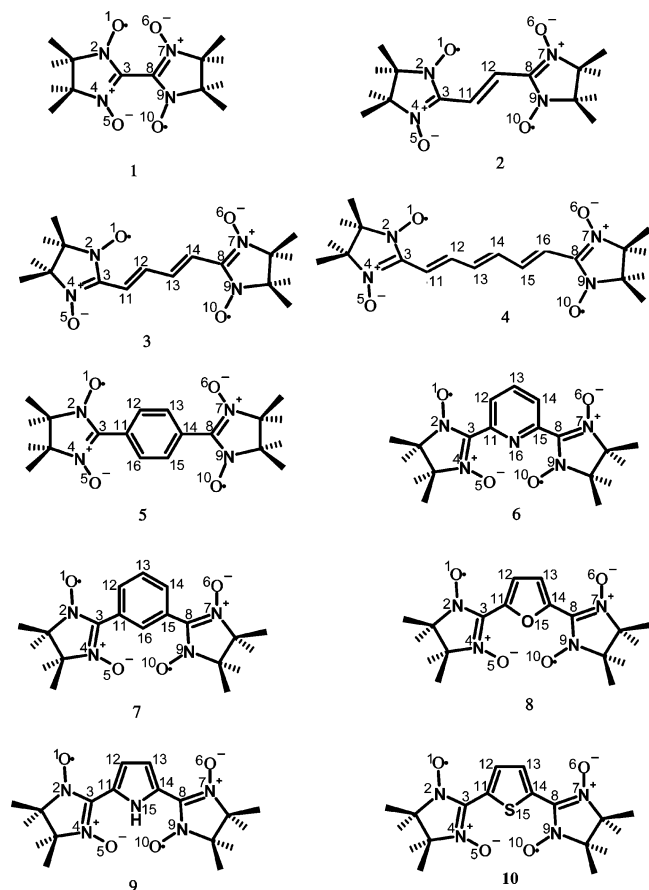


Figure 1. Systems under investigation with (1) no coupler, (2) ethylene coupler, (3) 1,4-butadiene coupler, (4) 1,6-hexatriene coupler, (5) *p*-phenylene coupler, (6) 2,6-pyridine coupler, (7) *m*-phenylene coupler, (8) 2,5-furan coupler, (9) 2,5-pyrrole coupler, and (10) 2,5-thiophene coupler between the two nitronyl nitroxide monoradicals.

erate NBMOs, with the prediction of a triplet ground state. However, in a variety of conjugated systems the Hund's criterion does not necessarily follow, and a singlet ground-state results. TME and its derivatives are the simplest examples of such system. The low-spin nature of TME and the related disjoint systems was explained by a VB-type electronic exchange. A number of derivations were made to model the intramolecular exchange in connectivity-conjugated systems by Ovchinnikov,¹² Klein,¹³ Borden and Davidson¹⁴ and Sinanoglu.¹⁵ In all these cases the simplistic MO theory and the Hund's rule do not follow in a proper way. A large number of computational studies have been performed on this issue.^{16–18} It is observed that the spin polarization argument is more useful to understand the spin density distribution in an open shell system.

In this work we have followed the spin-polarized DFT methodology to calculate the magnetic exchange coupling constants. The broken-symmetry (BS) approach that was proposed by Noodleman et al.¹⁹ has been adopted here.

This paper is organized as follows. In section 2 we briefly mention the salient features of the theoretical background. The computational methodologies are described in section 3. Section 4 contains a discussion of the results and the concluding remarks are given in section 5.

2. Theoretical Background

The magnetic exchange interaction between two magnetic sites 1 and 2 is normally expressed by the Heisenberg spin

Hamiltonian

$$\hat{H} = -2J\hat{S}_1 \cdot \hat{S}_2 \quad (1)$$

where \hat{S}_1 and \hat{S}_2 are the respective spin angular momentum operators. A positive sign of J indicates a ferromagnetic interaction, whereas the negative sign indicates an antiferromagnetic interaction. The eigenfunctions of the Heisenberg Hamiltonian are eigenfunctions of \hat{S}^2 and \hat{S}_z where S is the total spin angular momentum, and J is directly related to the energy difference between the spin eigenstates. For a diradical,

$$E(S=1) - E(S=0) = -2J \quad (2)$$

The Heisenberg description of the magnetic interaction can be correlated with the electronic structure of a given system.^{20–23} A large number ab initio calculations have been performed to evaluate J .²⁴ Nevertheless, a proper mapping between the Heisenberg spin eigenstates and suitable ab initio electronic states, especially the singlet states, is necessitated for the above procedure. This is computationally very expensive and not practical for large systems.

An alternative approach has been proposed by Noodleman so as to reliably compute the magnetic exchange coupling constant with less computational effort.¹⁹ The spin polarized, unrestricted formalism and a broken-symmetry solution is needed for the lowest spin-state in this method. The BS state is not an eigenstate of \hat{H} . It is an equal mixture of singlet and triplet states. The coupling constant can be written as

$$J = \frac{(E_{BS} - E_T)}{1 + S_{ab}^2} \quad (3)$$

where S_{ab} is the overlap integral between the two magnetic orbitals a and b . The quantity E_{BS} is the energy of the broken-symmetry solution and E_T is the energy of the triplet state in the unrestricted formalism using the BS orbitals. In a single-determinant approach, E_T can be approximated by the energy of the triplet state that is achieved by a direct computation ($E_T \approx E_T$), because of the very less spin contamination in the high-spin state. In contrast, the BS state is often found as spin-contaminated. Therefore, spin-projected methods have been applied to eliminate the effect of the spin contamination from the energy of the BS state. The following three equations (eqs 4–6) are the results obtained from these methods:

$$J^{(1)} = \frac{({}^{\text{DFT}}E_{BS} - {}^{\text{DFT}}E_T)}{S_{\text{max}}^2} \quad (4)$$

$$J^{(2)} = \frac{({}^{\text{DFT}}E_{BS} - {}^{\text{DFT}}E_T)}{S_{\text{max}}(S_{\text{max}} + 1)} \quad (5)$$

$$J^{(3)} = \frac{({}^{\text{DFT}}E_{BS} - {}^{\text{DFT}}E_T)}{\langle S^2 \rangle_T - \langle S^2 \rangle_{BS}} \quad (6)$$

These three relations differ in their applicability, which depends on the degree of overlap between the two magnetic orbitals. Equation 4 has been derived by Ginsberg,²⁵ Noodleman,¹⁹ and Davidson²⁶ (GND) and is applied when the overlap of the magnetic orbitals is sufficiently small. Equation 5 has been proposed by GND, Bencini et al.,²⁷ and Ruiz et al.²⁸ Illas et al.²⁹ have justified the application of eq 5 when the overlap is adequately large. Finally, eq 6 has been developed by Yamagu-

chi et al.³⁰ This can be reduced to eq 4 and eq 5 in the weak and strong overlap regions, respectively.

In this work we have explicitly computed the overlap integral S_{ab} . The α -HOMO and β -HOMO in the BS state have been considered as the magnetic orbitals. It is observed that the overlap between the magnetic orbitals is very low for all the diradicals except **1a**, **1c** and **1d**. We have further noticed that the $\langle S^2 \rangle$ value for all the calculated BS states deviate very little from 1.00, and, in particular, the difference ($\langle S^2 \rangle_T - \langle S^2 \rangle_{BS}$) is nearly equal to unity for the systems. Therefore, the magnetic exchange constants have been calculated here by using both eq 3 and eq 4. Only in the moderately large S_{ab} region, for **1a**, **1c**, **1d** and **2**, eq 3 is estimated to yield better result. All J values calculated from eqs 3–6 are given as Supporting Information.

3. Computational Strategy

The molecular structures of all the diradicals **1–10** have been fully optimized at the ROHF/6-31G(d,p) level. The optimized dihedral angle of diradical **1** between the two planes of the NN moiety has been found to be 78° in the isolated molecule. But the crystallographic data suggest that the dihedral angle is 55°. ³¹ So we have taken several values of the dihedral angle between the two NN moieties while keeping the rest of the optimized molecule intact, and computed the exchange coupling constant for each of these geometries. The angles considered are 0°, 55°, 78° and 90°.

Single point calculations have been performed on the optimized geometry at the UB3LYP level with 6-311G(d,p) and 6-311+G(d,p) basis sets. To obtain the broken-symmetry states, single-point UB3LYP calculations have been carried out using the accurate guess values of molecular orbitals, which are in turn retrieved from the proper ROHF calculations. These calculations have been done by using Gaussian 98 quantum chemical package.³² The visualization software Molden³³ and Molekel³⁴ have also been used. The overlap integral between the two magnetic orbitals in the BS state has been calculated by a program of our own. This program utilizes the MO coefficients and basis set information at 6-311+G(d,p) level from the Gaussian 98 log files.

To further support the magnetic properties, the hyperfine coupling constants (hfcc) have been calculated at B3LYP level by using EPR-II and EPR-III basis sets.³⁵ The diradical **10** contains one S atom, but this atom is not included in the EPR basis set of Gaussian 98. Therefore, during the calculation of hfcc we have used the 6-311G(d,p) basis set for the S atom, whereas EPR-II and EPR-III basis sets have been used for the rest of the atoms.

4. Results and Discussion

First of all, to make the discussion clear, the computed overlap integrals (S_{ab}) are given in Table 1. The moderately large overlap region is manifest for **1a**, **1c**, **1d** and **2**. For these species, neither (4) nor (5) can be used with accuracy. Therefore, eq 3 gives a better estimate of J value. For **1b** and **9**, eq 3 would make a deviation of about 3% and 2% respectively from the J value calculated from eq 4. For all others, eq 4 represents a better choice.

The calculation of the intramolecular exchange coupling constant between the two NN monoradicals without any coupler (in species **1**) is shown in Table 2. The J values for the planar diradicals with no coupler and π -conjugated linear couplers are tabulated in Table 3. The values for the six-membered and five-membered conjugated aromatic couplers are given in Tables 4 and 5, respectively.

TABLE 1: Computed Overlap Integral between the Two Magnetically Active Orbitals in Broken-Symmetry State^a

| SI no. | Coupler | S_{ab} |
|-----------|---------------------|-----------|
| 1a | 0° dihedral angle | -0.494041 |
| 1b | 55° dihedral angle | -0.178056 |
| 1c | 78° dihedral angle | -0.791540 |
| 1d | 90° dihedral angle | 0.569932 |
| 2 | ethelene | 0.361410 |
| 3 | 1,4-butadiene | 0.039911 |
| 4 | 1,6-hexatriene | -0.072483 |
| 5 | <i>p</i> -phenylene | -0.014067 |
| 6 | <i>m</i> -pyridine | 0.044348 |
| 7 | <i>m</i> -phenylene | -0.051216 |
| 8 | 2,5-furan | -0.006970 |
| 9 | 2,5-pyrrole | 0.134857 |
| 10 | 2,5-thiophene | 0.036758 |

^a The computed results are for the 6-311+G(d,p) basis sets.

Table 2 shows that the magnitude of J drastically decreases with the increase in the dihedral angle. The highest J is -923 cm^{-1} for the planar configuration, and the lowest value is -29 cm^{-1} for the 90° rotated species. This is due to the maximum overlap between the two p-orbitals in bridging carbon atoms when the dihedral angle is 0°, and the minimum conjugation when the two p-orbitals in bridging atoms are orthogonal. In crystal structure of **1** it is observed that the dihedral angle is 55°. The J value calculated for **1b** by using eq 4 excellently matches with the observed J in molecular crystals. The trend in Table 2 makes it amply clear that *the delocalization of the π -electrons plays the major role in controlling the exchange coupling constant*. The larger dihedral angle inhibits conjugation of the π -electrons. Nevertheless, a weak antiferromagnetic interaction exists even when the two p-orbitals are orthogonal to each other. In this case, there is a strong localization of the SOMOs. The spin of the unpaired electron in one of the π -orbitals polarizes the spin of the paired electrons in the orthogonal σ -orbital. *The residual spin polarization is the sole reason for a very weak antiferromagnetic coupling constant in 1d.*

It is observed that the exchange coupling constant decreases with the increase of the length of the coupler (Table 3). In this Table, eq 3 is a better description for **1a** and eq 4 is more appropriate for **2–4**. This is a very normal trend. It is observed that **2** has the highest J value. Our previous communication has also supported this finding.⁷ The main reason for it is that the steric effects force the dihedral angle of **1** to be 55° in molecular crystal, which causes loss of delocalization. The rule of spin alternation in the UHF treatment³⁶ can also predict the proper ground spin state for all the cases in Table 2 and Table 3 (Figure 2).

The calculated J values are in very good agreement with the observed values for **5–7** in Table 4. Here, we find hardly any difference between eqs 3 and 4. The length of the coupler in **5** is similar to the butadiene coupler in **3**. However, the magnetic exchange coupling constant is found to be less than that for the linear conjugated coupler. In general, all the conjugated aromatic couplers are weaker than the linear couplers. The spin alternation rule for the prediction of the ground-state spin is also followed by 1,4 phenylene (**5**),³⁷ 2,6-pyridine coupler (**6**)³⁸ and 2,6 phenylene coupler (**7**),³⁹ resulting in singlet, triplet and triplet ground states, respectively.

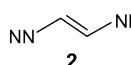
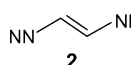
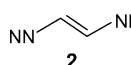
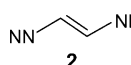
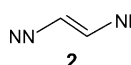
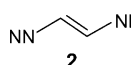
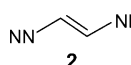
Results for **8–10** are given in Table 5. Here, again, the GND expression (4) gives a more reliable estimate of J in every case. The data for **5** have been included in this Table for the reason of making a facile comparison. The calculated J is in good agreement with the observed value for **10**.⁴⁰ Experimental values

TABLE 2: Single-Point Energies and Calculated Intramolecular Exchange Coupling Constants for the Nitronyl Nitroxide (NN) Diradicals without Any Coupler^a

| Dihedral angle | Basis sets | Energy (a.u.) ($\langle S^2 \rangle$) | | J (cm ⁻¹) | | |
|-------------------------------|------------|--|---------------|-------------------------|---------|-------------------|
| | | BS | T | Calculated | | Exptl |
| | | | | Eq. (3) | Eq. (4) | |
| 0° 1a | 6-311G** | -1067.7727349 | -1067.7675028 | -923 | -1148 | NA ^b |
| | | 1.125262 | 2.046992 | | | |
| 55° ^c 1b | 6-311+G** | -1067.7904005 | -1067.7851668 | -923 | -1148 | -311 ^d |
| | | 1.111334 | 2.046176 | | | |
| 78° ^e 1c | 6-311G** | -1067.8615782 | -1067.8602569 | -281 | -290 | -311 ^d |
| | | 1.077337 | 2.060998 | | | |
| 90° 1d | 6-311+G** | -1067.8806805 | -1067.8793779 | -277 | -286 | NA ^b |
| | | 1.07538 | 2.06042 | | | |
| 78° ^e 1c | 6-311G** | -1067.864504 | -1067.8642504 | -34 | -56 | NA ^b |
| | | 1.073739 | 2.066934 | | | |
| 90° 1d | 6-311+G** | -1067.8848812 | -1067.8845819 | -41 | -66 | NA ^b |
| | | 1.070904 | 2.064865 | | | |
| 90° 1d | 6-311G** | -1067.8637813 | -1067.8636461 | -23 | -30 | NA ^b |
| | | 1.072735 | 2.068682 | | | |
| 90° 1d | 6-311+G** | -1067.884201 | -1067.8840684 | -22 | -29 | NA ^b |
| | | 1.070115 | 2.066156 | | | |

^a The coupling constant J is calculated for different dihedral angles. All the single-point calculations are performed with the UB3LYP methodology for the broken-symmetry state as well as the triplet state. ^b Not available in the literature. ^c Rotating the N-C-C-N dihedral angle of fully optimized geometry to 55° so as to get a structure similar to the crystallographic one. ^d Reference 31. ^e Fully optimized geometry at ROHF/6-311G(d,p) level.

TABLE 3: Single-Point Energies and Calculated Intramolecular Exchange Coupling Constants for π -Conjugated Linear Couplers^a

| Diradical | Basis sets | Energy (a.u.) ($\langle S^2 \rangle$) | | J (cm ⁻¹) | | Exptl. |
|---|------------|--|---------------|-------------------------|---------|-------------------|
| | | BS | T | Calculated | Eq. (4) | |
| | | | | Eq. (3) | Eq. (4) | |
| NN-NN 1a | 6-311G** | -1067.7727349 | -1067.7675028 | -923 | -1148 | NA ^b |
| | | 1.125262 | 2.046992 | | | |
|  2 | 6-311+G** | -1067.7904005 | -1067.7851668 | -923 | -1148 | NA ^b |
| | | 1.111334 | 2.046176 | | | |
|  3 | 6-311G** | -1145.3113872 | -1145.3096214 | -343 | -388 | -350 ^c |
| | | 1.139187 | 2.066011 | | | |
|  4 | 6-311+G** | -1145.3287469 | -1145.3271496 | -310 | -350 | -350 ^c |
| | | 1.1286 | 2.0629 | | | |
|  5 | 6-311G** | -1222.7385572 | -1222.7374101 | -251 | -251 | NA ^b |
| | | 1.144146 | 2.084033 | | | |
|  6 | 6-311+G** | -1222.7589119 | -1222.7578636 | -230 | -230 | NA ^b |
| | | 1.134768 | 2.080213 | | | |
|  7 | 6-311G** | -1300.1675127 | -1300.1668185 | -151 | -152 | -66 ^d |
| | | 1.130756 | 2.083696 | | | |
|  8 | 6-311+G** | -1300.1870287 | -1300.1864071 | -135 | -136 | -66 ^d |
| | | 1.120468 | 2.078546 | | | |

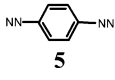
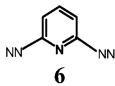
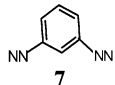
^a All the single-point calculations are performed with the UB3LYP methodology for the broken-symmetry state as well as the triplet state. Rotating the N-C-C-N dihedral angle of fully optimized geometry to 0° so as to get a planar structure like **2** and **3**. ^b Not available in the literature. ^c Reference 8a. ^d Reference 8b, for 1,6-dimethyl derivative.

are lacking for **8** and **9**, and the J values -148 and -164 cm⁻¹ are predicted estimates. Again, the spin alternation rule identifies the proper ground state for **10** as a singlet. The identified ground states for **8** and **9** are both singlet, in agreement with the computed J values.

The sign of J depends on the parity of the number of bonds in the coupling pathway through the coupler. When the number of bonds is odd, J is negative like in **1a**, **2**, **3** and **4** (1, 3, 5 and 7 bonds). In **5**, there are two five-bond coupling pathways (odd number) and the resulting J value is negative. In **6** and **7**, there

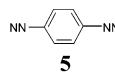
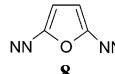
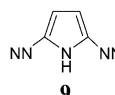
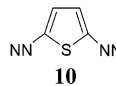
are two even coupling pathways (four- and six-bond couplings), and J is positive. These observations represent a mere restatement of the so-called spin alternation rule. In all three cases **8–10**, there are one even and one odd pathway. At a first glance, one would think that there is a competition between the two pathways. In reality, the odd (five-bond) route is supported by the even (four-bond) path through the heteroatom as the latter contributes two π electrons. The J values for **8–10** are all negative. In magnitude, these are actually larger than the J value for **5** (Table 5). This behavior is similar to that known for the

TABLE 4: Single-Point Energies and Calculated Intramolecular Exchange Coupling Constants for Aromatic Couplers^a

| Diradicals | Basis sets | Energy (a.u.) | | J (cm ⁻¹) | | Exptl. |
|--|------------|---------------------------|---------------------------|-------------------------|---------|------------------|
| | | BS | T | Calculated Eq. (3) | Eq. (4) | |
|  5 | 6-311G** | -1298.9901966 1.090979 | -1298.9897665 2.073425 | -94 | -94 | -72 ^b |
| | 6-311+G** | -1299.0106241 1.086835 | -1299.0102268 2.070655 | -87 | -87 | |
|  6 | 6-311G** | -1315.0163354 1.069793 | -1315.0164212 2.074852 | 19 | 19 | 7 ^c |
| | 6-311+G** | -1315.0289297 1.083623 | -1315.0290336 2.090128 | 23 | 23 | |
|  7 | 6-311G** | -1298.9864545 1.073124 | -1298.9865576 2.078921 | 23 | 23 | 20 ^d |
| | 6-311+G** | -1299.0066208 1.070268 | -1299.006716 2.075584 | 21 | 21 | |

^a All the single-point calculations are performed with the UB3LYP methodology for the broken-symmetry state as well as the triplet state. ^b Reference 37. ^c Reference 38. ^d Reference 39.

TABLE 5: Single-Point Energies and Calculated Intramolecular Exchange Coupling Constants for Five-Membered Aromatic Couplers^a

| Diradicals | Basis sets | Energy (a.u.) | | J (cm ⁻¹) | | Exptl. |
|---|------------|---------------------------|---------------------------|-------------------------|---------|-------------------|
| | | BS | T | Calculated Eq. (3) | Eq. (4) | |
|  5 | 6-311G** | -1298.9901966 1.090979 | -1298.9897665 2.073425 | -94 | -94 | -72 ^b |
| | 6-311+G** | -1299.0106241 1.086835 | -1299.0102268 2.070655 | -87 | -87 | |
|  8 | 6-311G** | -1296.7615506 1.098239 | -1296.760815 2.065873 | -161 | -161 | NA ^c |
| | 6-311+G** | -1296.7837161 1.092527 | -1296.7830414 2.062898 | -148 | -148 | |
|  9 | 6-311G** | -1276.9299062 1.100927 | -1276.9291011 2.07081 | -174 | -177 | NA ^c |
| | 6-311+G** | -1276.9503153 1.095613 | -1276.9495684 2.067769 | -161 | -164 | |
|  10 | 6-311G** | -1619.7607667 1.108292 | -1619.7599146 2.07297 | -187 | -187 | -157 ^d |
| | 6-311+G** | -1619.7811119 1.101501 | -1619.7803369 2.069521 | -170 | -170 | |

^a The *p*-phenylene diradical is included here for the purpose of making a comparison possible. All the single-point calculations are performed with the UB3LYP methodology for the broken-symmetry state as well as the triplet state. ^b Reference 37. ^c Not available in the literature. ^d Reference 40.

Fermi contact contribution to nuclear spin–spin couplings transmitted through the π -electronic system in conjugated compounds and can be viewed as an extension of the spin alternation rule to the case of heteronuclear aromatic couplers.

Rationalization. The spin density distribution in all the species investigated here is more or less (pairwise) symmetric for rotation by 180° around the principal axis (C_2). An understanding of the trend of the J values in each series can be obtained by writing^{4e}

$$J = \sum_{i=j} J_{ij} \rho_i \rho_j \quad (7)$$

where ρ_i is the spin density on the i th atom in the triplet state,

and J_{ij} is the exchange integral between the π -orbitals of the atoms i and j . The integral J_{ij} is strongest for atoms i and j being nearest neighbors. For a conjugated coupler of N atoms, there are $(N + 1)$ nearest neighbors. But the absolute magnitude of the atomic spin density approximately varies as $1/(N + 1)$. Therefore, as N increases, the absolute magnitude of J decreases approximately as $1/(N + 1)$. This is a general trend, and Table 3 bears a glowing testimony to it. The trend is clearly set with $|J|$ exhibiting the order **1a** > **2** > **3** > **4** in the approximate ratio 1:1/3:1/5:1/7, and the longer the coupler is, the less antiferromagnetic interaction is there.

In the case of six-membered ring aromatic couplers, the rule of spin alternation indicates that an antiferromagnetic coupling

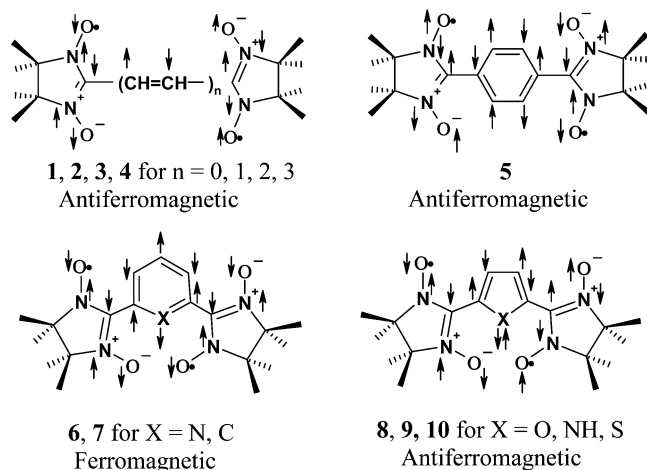


Figure 2. Prediction of ground spin states and hence the nature of the magnetic exchange coupling constants shown according to the spin alternation rule.

exists for *o*-phenylene and *p*-phenylene or their derivatives, and a ferromagnetic coupling exists for *m*-phenylene. For five-membered ring heteronuclear aromatic couplers, the 2,3 and 3,4 species are to be treated as the *o*-couplers, the 2,5 species is a *p*-coupler and the 2,4 one as an *m*-coupler, because the heteroatom at 1 provides two π -electrons.

The chain rule here suggests that $J \propto 2(N+1)/(2N+1)$,² where $2N$ is the number of conjugated atoms in the coupler. Thus, $J \propto 8/49$ for six-membered *p*-couplers whereas $J \propto 1/5$ for the butadiene coupler. Therefore, the magnitude of the J value decreases by ring formation. The atomic spin densities in the coupler decrease further due to resonance. So a six-membered π -coupler has a considerably reduced $|J|$ compared to the value for a linear chain of 4 carbon atoms. This is turned out by the calculated values for the butadiene coupler **3** (-230 cm^{-1}) in Table 3 and the *p*-phenylene coupler **5** (-87 cm^{-1}) in Table 4. For the six-membered *m*-couplers such as **6** and **7**, as aromaticity increases, the J value increases (Table 4). Therefore, aromaticity favors the ferromagnetic trend.

The heteronuclear couplers are less aromatic. Therefore, by counting all the six π electrons, the para coupling with heteronuclear aromatic spacers would entail $J \propto 1/5$. But the resonance decreases the atomic spin densities. These two factors lead to a J value that is almost midway between the J for **3** (-230 cm^{-1}) and the J for **5** (-87 cm^{-1}). See Table 5. Here again, the decrease in aromaticity is accompanied by an increase in antiferromagnetic coupling. This is evidenced from the trend $5 < 8 < 9 < 10$ for the absolute magnitude of the calculated J values given in the same table.

SOMO–SOMO Energy Level Splitting. Hoffmann⁴¹ provided a criterion based on the extended Hückel calculations on benzyne and diradicals, which suggests that if the energy difference between the two SOMOs (ΔE_{SS}) is less than 1.5 eV, the two nonbonding electrons will occupy different degenerate orbitals with a parallel-spin configuration so as to minimize their electrostatic repulsion and thereby leading to a triplet ground state. Constantinides et al.⁴² have investigated a series of $4n\pi$ antiaromatic linear and angular poly-heteroacene molecules by B3LYP/6-31G(d) method and found that singlet ground states result when $\Delta E_{SS} > 1.3 \text{ eV}$. Zhang et al.⁴³ have calculated a series of *m*-phenylene-bridged diradicals to investigate the effect of substitution on the S–T energy gaps and ground-state multiplicity. They have calculated ΔE_{SS} at the ROB3LYP/6-31G(d) level. The low spin ground-state results even when ΔE_{SS} is found to be 0.19 eV. Our calculation of ΔE_{SS} for all the

TABLE 6: Energy Levels of Two SOMOs and Their Energy Differences (ΔE_{SS}) at the ROB3LYP/6-311+G(d,p) Level for the Diradicals 1–10

| Diradicals | $E_S(1)$ (a.u.) | $E_S(2)$ (a.u.) | ΔE_{SS} (eV) |
|------------|-----------------|-----------------|----------------------|
| 1a | −0.08364 | −0.11228 | 0.7793 |
| 1b | −0.09236 | −0.09764 | 0.1437 |
| 1c | −0.09701 | −0.09850 | 0.0405 |
| 1d | −0.09818 | −0.09837 | 0.0052 |
| 2 | −0.09405 | −0.09550 | 0.0395 |
| 3 | −0.09599 | −0.09625 | 0.0071 |
| 4 | −0.09647 | −0.09662 | 0.0041 |
| 5 | −0.09393 | −0.09410 | 0.0046 |
| 6 | −0.09189 | −0.09590 | 0.1091 |
| 7 | −0.09272 | −0.09661 | 0.1059 |
| 8 | −0.09656 | −0.09680 | 0.0065 |
| 9 | −0.09670 | −0.09681 | 0.0030 |
| 10 | −0.09709 | −0.09764 | 0.0150 |

diradicals **1–10** by ROB3LYP/6-311+G(d,p) method in Table 6 does not reveal much information about the ground-state spin.

For the diradicals **1a–1d** the SOMO–SOMO energy gap decreases as the dihedral angle increases. Thus the magnitude of the J value decreases with the decrease of the SOMO–SOMO energy gap. This trend is in agreement with the Hay–Thibeault–Hoffmann (HTH) formula for the triplet–singlet energy difference⁴⁴ in a dinuclear complex containing two weakly interacting metal atoms in a dinuclear complex. For species **1**, the SOMOs are not degenerate even when the *p*-orbitals are orthogonal to each other. A very weak antiferromagnetic interaction is observed in species **1d**. However, as Table 6 shows, the same formula does not hold for other diradicals examined here: species **6** and **7** with relatively large SOMO–SOMO energy gaps are known to have ferromagnetic coupling^{38,39} and our calculations also support this fact (Table 4), whereas the others have much smaller gaps but are antiferromagnetically coupled.

The shape of all the SOMOs at ROB3LYP for diradicals **1–10** are given in Figure 3. In general, two types of SOMOs are found, namely, disjoint (where no atoms are common) and nondisjoint (with common atoms). All the diradicals except **6** and **7** are nondisjoint in nature. The SOMOs of **2** and **9** seem to be apparently disjoint, but these are in reality nondisjoint as observed from the molecular orbital coefficients. We find that for the type of organic diradicals studied here, the ferromagnetic interaction arises when the shapes of the SOMOs are disjoint in nature as in **6** and **7** (Figure 3).

A similar point of interest arises. Borden and Davidson had argued that if Hückel NBMO's are not localized to disjoint groups of atoms, the triplet would lie below the corresponding open-shell singlet at the SCF level.¹⁴ Our results contradict this observation but are in good agreement not only with experiment (Table 4) but also with the prediction from the rule of spin alternation.

Isotropic Hyperfine Coupling Constant. From the experimental work it is observed that the hfcc of the two equivalent nitrogen atoms in nitronyl nitroxide monoradicals with different substitutions at α -carbon atoms is in the range of 7.00–7.81 G.⁴⁵ The hfcc does not strongly depend on the nature of the substitution at the α -position, but solvents play a dominant role. Hfcc values for diradicals with conjugated couplers decrease to half of the values for the corresponding monoradicals. The experimental values lie in the range of 3–4.5 G for diradicals with different couplers.⁴⁶

Cirujeda et al.⁴⁷ calculated the hfcc for several α -nitronyl aminoxy radicals by B3LYP method using EPR-II basis sets.

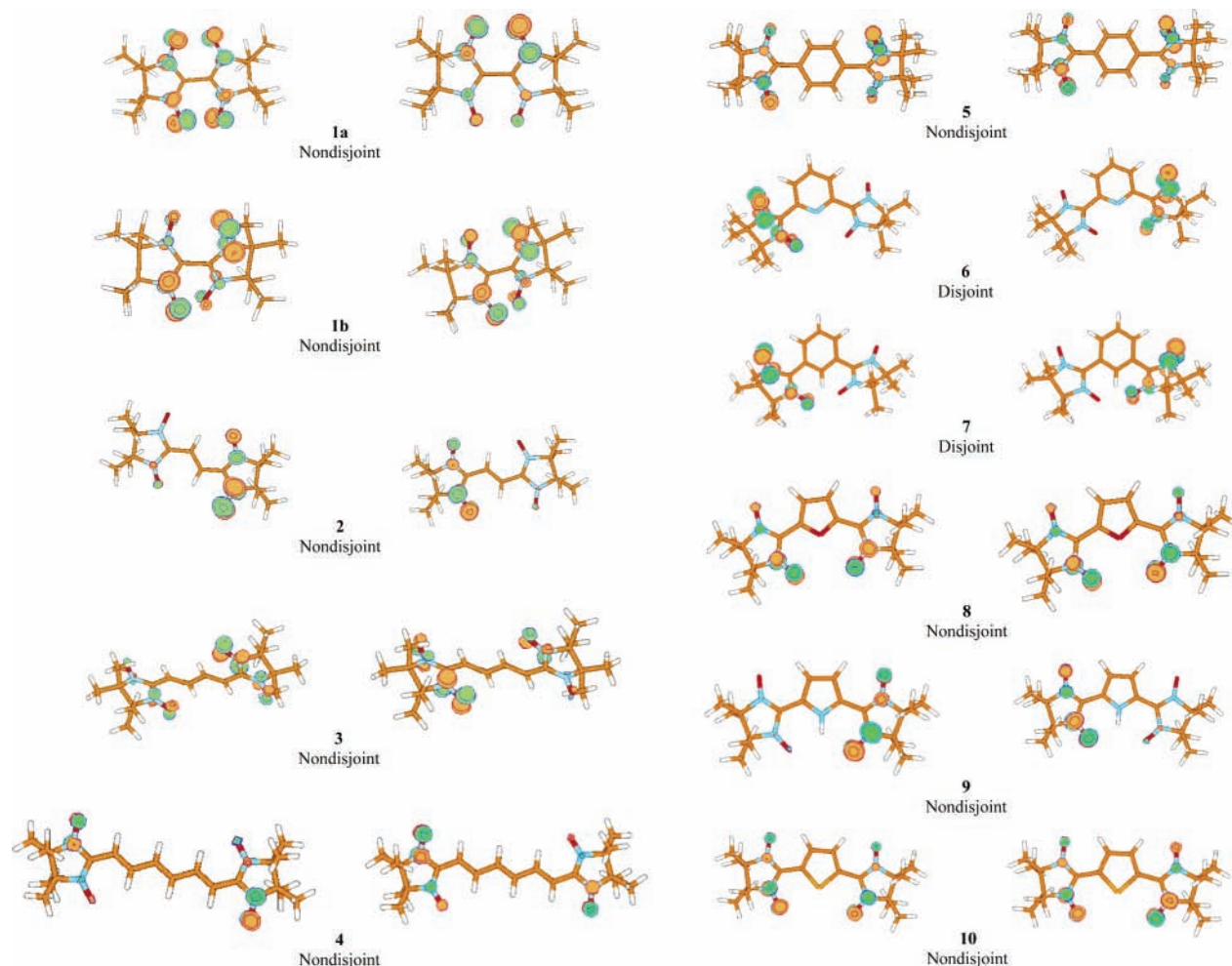


Figure 3. Triplet SOMOs for all the diradicals 1–10, plotted at the ROB3LYP/6-311+G(d,p) level.

TABLE 7: Highperfine Coupling Constants (hfcc) Calculated at B3LYP Level with EPR-II and EPR-III Basis Sets

| Diradicals | Basis sets | a_{N2} (G) | a_{N4} (G) | a_{N7} (G) | a_{N9} (G) | Obsd a_N |
|------------|------------|--------------|--------------|--------------|--------------|------------------|
| 1a | EPR-II | 4.11025 | 1.04162 | 1.03287 | 4.16915 | |
| | EPR-III | 4.23427 | 1.15317 | 1.14087 | 4.29395 | |
| 1b | EPR-II | 4.31866 | 1.06099 | 1.05223 | 4.38357 | |
| | EPR-III | 4.47133 | 1.21081 | 1.20199 | 4.53641 | |
| 1c | EPR-II | 4.46136 | 1.06774 | 1.07244 | 4.39365 | |
| | EPR-III | 4.67802 | 1.12935 | 1.13714 | 4.60911 | |
| 1d | EPR-II | 4.59041 | 1.02385 | 1.03317 | 4.52136 | |
| | EPR-III | 4.73748 | 1.17743 | 1.18690 | 4.66801 | |
| 2 | EPR-II | 4.52596 | 1.50349 | 1.34520 | 4.44834 | |
| | EPR-III | 4.17437 | 1.77937 | 1.49466 | 4.23153 | |
| 3 | EPR-II | 4.35821 | 1.71624 | 1.71544 | 4.35549 | |
| | EPR-III | 4.43620 | 1.73844 | 1.73774 | 4.43366 | |
| 4 | EPR-II | 4.54130 | 1.72502 | 1.72495 | 4.54584 | |
| | EPR-III | 4.50506 | 1.80138 | 1.80096 | 4.50906 | |
| 5 | EPR-II | 3.38184 | 1.65462 | 1.65528 | 3.38509 | |
| | EPR-III | 3.50442 | 1.74658 | 1.74706 | 3.50721 | |
| 6 | EPR-II | 4.48825 | 1.66194 | 1.66113 | 4.44737 | 3.3 ^a |
| | EPR-III | 4.59373 | 1.66533 | 1.66506 | 4.55285 | |
| 7 | EPR-II | 3.51368 | 1.49883 | 1.44803 | 4.62565 | |
| | EPR-III | 3.76404 | 1.84418 | 1.80126 | 4.88496 | |
| 8 | EPR-II | 4.83269 | 1.62270 | 1.62222 | 4.83306 | |
| | EPR-III | 4.94187 | 1.65987 | 1.65902 | 4.94245 | |
| 9 | EPR-II | 3.78055 | 1.48492 | 1.46878 | 4.86759 | |
| | EPR-III | 3.92236 | 1.66391 | 1.64693 | 5.01510 | |
| 10 | EPR-II | 4.33239 | 1.50318 | 1.50422 | 4.30763 | 3.7 ^b |
| | EPR-III | 4.51469 | 1.59648 | 1.59748 | 4.48928 | |

^a Reference 38. ^b Reference 40.

They found similar hfcc for the monoradicals with similar steric constraints between the two rings. This fact also supports that the spin density distribution in the phenyl ring is not strongly

dependent on the nature and position of substituents. In our previous work a detailed discussion was given on this issue.⁴⁸

Table 7 shows that although the computed hfccs are different for the four nitrogen atoms in diradicals 1–10. The average hfcc is reliably generated. A similar discrepancy was also found by other authors. From the spin density distribution in the triplet state it is observed that the calculated spin density is not homogeneously distributed through the O–N–C–N–O bond, though the two N atoms are chemically equivalent. This fact results in different values of hfcc and is supported by the SOMO's in Figure 3 and spin density distribution table given in Supporting Information.

5. Conclusions

A series of bis-nitrotronyl nitroxide diradicals with 10 different conjugated couplers have been investigated by broken-symmetry density functional treatment. The computed magnetic exchange coupling constants are in very good agreement with the reported values. Moreover, J values for 3, 4, 8 and 9 are predicted here, (-230 , -136 , -148 and -161 cm^{-1} , respectively)

Sometimes it becomes necessary to explicitly compute the overlap integral between the two magnetically active orbitals to calculate the exchange coupling constant accurately by the broken-symmetry approach. The α -HOMO and β -HOMO in the BS state are generally found to be magnetic orbitals.

In conjugated systems, the magnetic interaction is mainly transmitted through the π -electron conjugation.

The strength of antiferromagnetic interaction decreases with the increase in the length of conjugated couplers. Conjugated linear couplers are more efficient antiferromagnetic couplers than the aromatic ones of similar length. As the aromaticity of the spacer decreases, the magnitude of the antiferromagnetic coupling constant increases. In general, aromaticity favors the ferromagnetic trend. The diradicals with *m*-couplers are undoubtedly ferromagnetic. The shape of the SOMOs as well as the rule of spin alternation in the UHF emerge as two robust guidelines for the prediction of the qualitative nature of the intramolecular magnetic interaction in bis-nitronyl nitroxide diradicals.

Acknowledgment. S.N.D. gratefully acknowledges financial support from the Department of Science and Technology and the computational facility of Galaxy cluster at the Department of Aerospace.

Supporting Information Available: Table of comparison of all the *J* values calculated from eqs 3–6, tables of spin density for all the species and the optimized coordinates of all the 10 diradicals. This material is available free of charge via the Internet at <http://pubs.acs.org>.

References and Notes

- (1) Tamura, M.; Nakazawa, Y.; Shiomi, D.; Nozawa, K.; Hosokoshi, Y.; Ishikawa, M.; Takahashi, M.; Kinoshita, M. *Chem. Phys. Lett.* **1991**, *186*, 401.
- (2) Nakazawa, Y.; Tamura, M.; Shirakawa, N.; Shiomi, D.; Takahashi, M.; Kinoshita, M.; Ishikawa, M. *Phys. Rev. B* **1992**, *46*, 8906.
- (3) (a) Takui, T.; Sato, K.; Shiomi, D.; Ito, K.; Nishizawa, M.; Itoh, K. *Synth. Met.* **1999**, *103*, 2271. (b) Romero, F. M.; Ziessel, R.; Bonnet, M.; Pontillon, Y.; Ressouche, E.; Schweizer, J.; Delley, B.; Grand, A.; Paulsen, C. *J. Am. Chem. Soc.* **2000**, *122*, 1298. (c) Nagashima, H.; Irisawa, M.; Yoshioka, N.; Inoue, H. *Mol. Cryst. Liq. Cryst. Sci. Technol. Sect. A* **2002**, *376*, 371. (d) Rajadurai, C.; Ivanova, A.; Enkelmann, V.; Baumgarten, M. *J. Org. Chem.* **2003**, *68*, 9907. (e) Wautelet, P.; Le Moigne, J.; Videva, V.; Turek, P. *J. Org. Chem.* **2003**, *68*, 8025. (f) Deumal, M.; Robb, M. A.; Novoa, J. *J. Polyhedron* **2003**, *22* (14–17), 1935.
- (4) (a) Kahn, O. *Molecular Magnetism*; VCH: New York, 1993. (b) Goodenough J. B. *Magnetism and the Chemical Bond*; Interscience: New York, 1963. (c) Coronado, E.; Delhaè, P.; Gatteschi, D.; Miller, J. S. *Molecular Magnetism: From Molecular Assemblies to the Devices*; Nato ASI Series E, Applied Sciences; Kluwer Academic Publisher: Dordrecht, The Netherlands, 1996; Vol. 321. (d) Benelli, C.; Gatteschi, D. *Chem. Rev.* **2002**, *102*, 2369. (e) McConnell, H. M. *J. Chem. Phys.* **1958**, *28*, 1188.
- (5) (a) Wautelet, P.; Catala, L.; Bieber, A.; Turek, P.; André, J.-J. *Polyhedron* **2001**, *20*, 1571. (b) Catala, L.; Moigne, J. L.; Kyritsakas, N.; Rey, P.; Novoa, J. J.; Turek, P. *Chem. Eur. J.* **2001**, *7*, 2466. (c) Wautelet, P.; Le Moigne, J.; Videva, V.; Turek, P. *J. Org. Chem.* **2003**, *68*, 8025. (d) Catala, L.; Le Moigne, J.; Gruber, N.; Novoa, J. J.; Rabu, P.; Belorizky, E.; Turek, P. *Chem. Eur. J.* **2005**, *11*, 2400.
- (6) Castell, O.; Caballol, R.; Subra, R.; Grand, A. *J. Phys. Chem.* **1995**, *99*, 154.
- (7) Barone, V.; Bencini, A.; Matteo, A. di. *J. Am. Chem. Soc.* **1997**, *119*, 10831.
- (8) (a) Ziessel, R.; Stroh, C.; Heise, H.; Köehler, F. K.; Turek, P.; Claiser, N.; Souhassou, M.; Lecomte, C. *J. Am. Chem. Soc.* **2004**, *126*, 12604. (b) Stroh, C.; Ziessel, R.; Raudaschl-Sieber, G.; Köehler, F.; Turek, P. *J. Mater. Chem.* **2005**, *15*, 850.
- (9) Vyas, S.; Ali, Md. E.; Hossain, E.; Patwardhan, S.; Datta, S. N. *J. Phys. Chem. A* **2005**, *109*, 4213.
- (10) Dietz, F.; Tyutyulkov, N. *Chem. Phys.* **2001**, *264*, 37.
- (11) (a) Lahti, P. M.; Ichimura, A. S. *J. Org. Chem.* **1991**, *56*, 3030. (b) Ling, C.; Minato, M.; Lahti, P. M.; van Willigen, H. *J. Am. Chem. Soc.* **1992**, *114*, 4, 9959. (c) Minato, M.; Lahti, P. M. *J. Am. Chem. Soc.* **1997**, *119*, 2187.
- (12) Ovchinnikov, A. A. *Theor. Chim. Acta* **1978**, *47*, 297.
- (13) (a) Klein, D. *J. Pure Appl. Chem.* **1983**, *55*, 299. (b) Klein, D. J.; Alexander, S. A. In *Graph Theory and Topology in Chemistry*; King, R. B., Rouvay, D. H., Eds.; Elsevier: Amsterdam, The Netherlands, 1987; Vol. 51, p 404.
- (14) Borden, W. T.; Davidson, E. R. *J. Am. Chem. Soc.* **1977**, *99*, 4587.
- (15) Shen, M.; Sinanoğlu, O. In *Graph Theory and Topology in Chemistry*; King, R. B., Rouvay, D. H., Eds.; Elsevier: Amsterdam, The Netherlands, 1987; Vol. 51, p 373.
- (16) (a) Nachtigall, P.; Jordan, K. D. *J. Am. Chem. Soc.* **1992**, *114*, 4743. (b) Nachtigall, P.; Jordan, K. D. *J. Am. Chem. Soc.* **1993**, *115*, 270.
- (17) Rijkenberg, R. A.; Buma, W. J.; van Walree, C. A.; Jennekens, L. W. *J. Phys. Chem. A* **2002**, *106*, 5249.
- (18) Datta, S. N.; Mukherjee, P.; Jha, P. P. *J. Phys. Chem. A* **2003**, *107*, 5049.
- (19) (a) Noodleman, L. *J. Chem. Phys.* **1981**, *74*, 5737. (b) Noodleman, L.; Baerends, E. J. *J. Am. Chem. Soc.* **1984**, *106*, 2316. (c) Noodleman, L.; Peng, C. Y.; Case, D. A.; Mouesca, J.-M. *Coord. Chem. Rev.* **1995**, *144*, 199.
- (20) (a) Heisenberg, W. *Z. Phys.* **1928**, *49*, 619. (b) Dirac, P. A. M. *The Principles of Quantum Mechanics*, 3rd ed.; Clarendon: Oxford, U.K., 1947.
- (21) (a) Nesbet, R. K. *Ann. Phys.* **1958**, *4*, 87. (b) Nesbet, R. K. *Phys. Rev.* **1960**, *119*, 658.
- (22) (a) Anderson, P. W. *Phys. Rev.* **1959**, *115*, 5745. (b) Anderson, P. W. *Solid State Phys.* **1963**, *14*, 99.
- (23) (a) Herring, C. In *Magnetism*; Rado, G. T., Shul, H., Eds.; Academic Press: New York, 1965; Vol. 2B. (b) Maynau, D.; Durand, Ph.; Daudey, J. P.; Malrieu, J. P. *Phys. Rev. A* **1983**, *28*, 3193.
- (24) (a) De Loth, P.; Cassoux, P.; Daudey, J. P.; Malrieu, J. P. *J. Am. Chem. Soc.* **1981**, *103*, 4007. (b) Miralles, J.; Castell, O.; Caballol, R. *Chem. Phys.* **1994**, *179*, 377. (c) Handrick, K.; Malrieu, J. P.; Castell, O. *J. Chem. Phys.* **1994**, *101*, 2213. (d) Wang, C.; Fink, K.; Staemmler, V. *Chem. Phys.* **1995**, *192*, 25. (e) Calzado, C. J.; Cabrero, J.; Malrieu, J. P.; Caballol, R. *J. Chem. Phys.* **2002**, *116*, 3985. (f) Calzado, C. J.; Cabrero, J.; Malrieu, J. P.; Caballol, R. *J. Chem. Phys.* **2002**, *116*, 2728. (g) Ciofini, I.; Daul, C. A. *Coord. Chem. Rev.* **2003**, *238*–239, 187.
- (25) Ginsberg, A. P. *J. Am. Chem. Soc.* **1980**, *102*, 111.
- (26) Noodleman, L.; Davidson, E. R. *Chem. Phys.* **1986**, *109*, 131.
- (27) (a) Bencini, A.; Totti, F.; Daul, C. A.; Doclo, K.; Fantucci, P.; Barone, V. *Inorg. Chem.* **1997**, *36*, 5022. (b) Bencini, A.; Gatteschi, D.; Totti, F.; Sanz, D. N.; McCleverty, J. A.; Ward, M. D. *J. Phys. Chem. A* **1998**, *102*, 10545.
- (28) Ruiz, E.; Cano, J.; Alvarez, S.; Alemany, P. *J. Comput. Chem.* **1999**, *20*, 1391.
- (29) (a) Martín, R. L.; Illas, F. *Phys. Rev. Lett.* **1997**, *79*, 1539. (b) Caballol, R.; Castell, O.; Illas, F.; Moreira, I. de P. R.; Malrieu, J. P. *J. Phys. Chem. A* **1997**, *101*, 7860. (c) Barone, V.; Matteo, A. de; Mele, F.; Moreira, I. de P. R.; Illas, F. *Chem. Phys. Lett.* **1999**, *302*, 240. (d) Illas, F.; Moreira, I. de P. R.; Graaf, C. de; Barone, V. *Theor. Chem. Acc.* **2000**, *104*, 265. (e) Graaf, C. de; Sousa, C.; Moreira, I. de P. R.; Illas, F. *J. Phys. Chem. A* **2001**, *105*, 11371.
- (30) (a) Yamaguchi, K.; Takahara, Y.; Fueno, T.; Nasu, K. *Jpn. J. Appl. Phys.* **1987**, *26*, L1362. (b) Yamaguchi, K.; Jensen, F.; Dorigo, A.; Houk, K. N. *Chem. Phys. Lett.* **1988**, *149*, 537. (c) Yamaguchi, K.; Takahara, Y.; Fueno, T.; Houk, K. N. *Theo. Chim. Acta* **1988**, *73*, 337.
- (31) Alies, F.; Luneau, D.; Laugier, J.; Rey, P. *J. Phys. Chem.* **1993**, *97*, 2922.
- (32) Frisch, M. J.; Trucks, G. W.; Schlegel, H. B.; Scuseria, G. E.; Robb, M. A.; Cheeseman, J. R.; Zakrzewski, V. G.; Montgomery, J. A., Jr.; Stratmann, R. E.; Burant, J. C.; Dapprich, S.; Millam, J. M.; Daniels, A. D.; Kudin, K. N.; Strain, M. C.; Farkas, O.; Tomasi, J.; Barone, V.; Cossi, M.; Cammi, R.; Mennucci, B.; Pomelli, C.; Adamo, C.; Clifford, S.; Ochterski, J.; Petersson, G. A.; Ayala, P. Y.; Cui, Q.; Morokuma, K.; Malick, D. K.; Rabuck, A. D.; Raghavachari, K.; Foresman, J. B.; Cioslowski, J.; Ortiz, J. V.; Stefanov, B. B.; Liu, G.; Liashenko, A.; Piskorz, P.; Komaromi, I.; Gomperts, R.; Martin, R. L.; Fox, D. J.; Keith, T.; Al-Laham, M. A.; Peng, C. Y.; Nanayakkara, A.; Gonzalez, C.; Challacombe, M.; Gill, P. M. W.; Johnson, B. G.; Chen, W.; Wong, M. W.; Andres, J. L.; Head-Gordon, M.; Replogle, E. S.; Pople, J. A. *Gaussian 98*; Gaussian, Inc.: Pittsburgh, PA, 1998. *Gaussian 98 for Windows*; Gaussian Inc.: Pittsburgh, 2002.
- (33) Schaftenaar, G.; Noordik, J. H. Molden: a pre- and post-processing program for molecular and electronic structures. *J. Comput.-Aided Mol. Design* **2000**, *14*, 123.
- (34) Flükiger, P.; Lüthi, H. P.; Portann, S.; Weber, J. *MOLEKEL*; v.4.3; Scientific Computing: Manno, Switzerland, 2002–2002. Portman, S.; Lüthi, H. P. *CHIMIA* **2000**, *54*, 766.
- (35) Barone, V. *Recent Advances in Density Functional Methods*; Chong, D. P., Ed.; World Scientific Publishing Co.: Singapore, 1996; Part I.
- (36) (a) Trindle, C.; Datta, S. N. *Int. J. Quantum Chem.* **1996**, *57*, 781. (b) Trindle, C.; Datta, S. N.; Mallik, B. *J. Am. Chem. Soc.* **1997**, *119*, 12947.
- (37) Caneschi, A.; Chiesi, P.; David, L.; Ferraro, F.; Gatteschi, D.; Sessoli, R. *Inorg. Chem.* **1993**, *32*, 1445.
- (38) Ziessel, R.; Ulrich, G.; Lawson, R. C.; Echegoyen, L. *J. Mater. Chem.* **1999**, *9*, 1435.
- (39) Shiomi, D.; Tamura, M.; Sawa, H.; Kato, K.; Kinoshita, H. *Synth. Met.* **1993**, *56*, 3279.
- (40) Mitsumori, T.; Inoue, K.; Koga, N.; Iwamura, H. *J. Am. Chem. Soc.* **1995**, *117*, 2467.
- (41) Hoffmann, R.; Zeiss, G. D.; Van Dine, G. W. *J. Am. Chem. Soc.* **1968**, *90*, 1485.

- (42) Constantinides, C. P.; Koutentis, P. A.; Schatz, J. *J. Am. Chem. Soc.* **2004**, *126*, 16232.
- (43) Zhang, G.; Li, S.; Jiang, Y. *J. Phys. Chem. A* **2003**, *107*, 5373.
- (44) Hay, P. J.; Thibeault, C. J.; Hoffmann, R. *J. Am. Chem. Soc.* **1975**, *97*, 4884.
- (45) (a) D'Anna, J. A.; Wharton, J. H. *J. Chem. Phys.* **1970**, *53*, 4047. (b) Jurgens, O.; Cirujeda, J.; Mas, M.; Mata, I.; Cabrero, A.; Vidal-Gancedo, J.; Rovira, C.; Molins, E.; Veciana, J. *J. Mater. Chem.* **1997**, *7*, 1723. (c) Zeissel, R.; Ulrich, G.; Lawson, R. C.; Echegoyen, L. *J. Mater. Chem.* **1999**, *9*, 1435. (d) Shiomi, D.; Sato, K.; Takui, T.; Itoh, K.; Tamura, M.; Nishio, Y.; Kajita, K.; Nakagawa, M.; Ishida, T.; Nogami, T. *Mol. Cryst. Liq. Cryst.* **1999**, *335*, 359.
- (46) (a) Luckhurst, G. R. In *Spin Labeling. Theory and applications*; Berliner, J. L., Ed.; Academic Press: New York, 1976; p 133 ff. (b) Luckhurst, G. R.; Pedulli, G. F. *J. Am. Chem. Soc.* **1970**, *92*, 4738; (c) Dulog, L.; Kim, J. S. *Makromol. Chemie* **1989**, *190*, 2609.
- (47) Cirujeda, J.; Vidal-Gancedo, J.; Jürgens, O.; Mota, F.; Novoa, J. J.; Rovira, C.; Veciana, J. *J. Am. Chem. Soc.* **2000**, *122*, 11393.
- (48) Ali, Md. E.; Vyas, S.; Datta, S. N. *J. Phys. Chem. A* **2005**, *109*, 6272.